

RESEARCH

Open Access



# DNA hypermethylation of *PLTP* mediated by DNMT3B aggravates vascular dysfunction in diabetic retinopathy via the AKT/GSK3 $\beta$ signaling pathway

Chunyang Cai<sup>1,2,3†</sup>, Chufeng Gu<sup>4\*†</sup>, Chunren Meng<sup>5†</sup>, Yujie Wang<sup>6†</sup>, Qingquan Wei<sup>1,9</sup>, Shuai He<sup>1</sup>, Dongwei Lai<sup>1,2,3</sup>, Xingyun Wang<sup>7\*</sup>, Tengfei Wang<sup>1,7\*</sup> and Qinghua Qiu<sup>1,8,9\*</sup>

## Abstract

**Background** This study aims to elucidate the effect and mechanism of phospholipid transfer protein (PLTP) on vascular dysfunction in DR and explore the molecular mechanism of abnormal PLTP expression based on DNA methylation.

**Methods** Human retinal microvascular endothelial cells (HRMECs) cultured in high glucose (HG) and streptozotocin-treated mice were used as DR models to detect and screen the key genes with abnormal promoter DNA methylation. Single-cell sequencing, tube formation and migration assays were employed to verify the relationship between PLTP and vascular function. Additionally, siRNA and luciferase reporter assay were used to study the key enzymes regulating the DNA methylation of *PLTP*. Transcriptome sequencing, coimmunoprecipitation and GSK3 $\beta$  inhibitor were utilized to identify and validate the key downstream pathways of PLTP.

**Results** DR models exhibited DNA hypermethylation and decreased expression of *PLTP*. Abnormal PLTP expression was implicated in vascular dysfunction, and *PLTP* overexpression reversed HG-induced effects on the migration and tube formation of endothelial cells. The siDNMT3B and luciferase reporter assay indicated that DNMT3B is the primary enzyme affecting abnormal methylation. Interestingly, PLTP promoted the phosphorylation of AKT and GSK3 $\beta$ , indicating that PLTP modulates angiogenesis via the AKT/GSK3 $\beta$  signaling pathway.

**Conclusions** PLTP regulates the proliferation, migration and tube formation of HRMECs, and is involved in maintaining vascular function via the AKT/GSK3 $\beta$  signaling pathway. In HG environment, increased DNMT3B expression upregulates DNA methylation of the *PLTP* promoter, downregulating PLTP expression and leading to vascular dysfunction in DR.

<sup>†</sup>Chunyang Cai, Chufeng Gu, Chunren Meng and Yujie Wang have contributed equally to this work.

\*Correspondence:

Chufeng Gu  
guchufeng@fjssl.com.cn  
Xingyun Wang  
wxy@shsmu.edu.cn  
Tengfei Wang  
wangtengfei2024@163.com  
Qinghua Qiu  
qinghuaqiu@163.com

Full list of author information is available at the end of the article

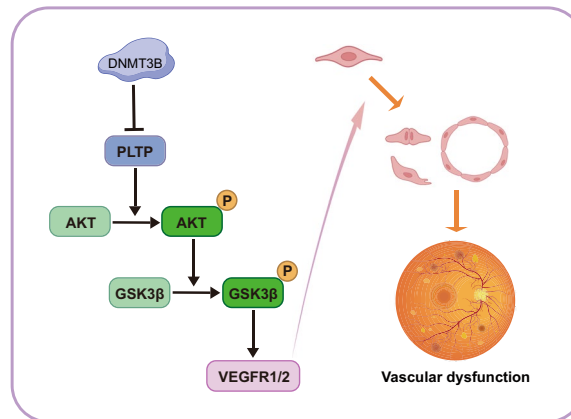


© The Author(s) 2025. **Open Access** This article is licensed under a Creative Commons Attribution-NonCommercial-NoDerivatives 4.0 International License, which permits any non-commercial use, sharing, distribution and reproduction in any medium or format, as long as you give appropriate credit to the original author(s) and the source, provide a link to the Creative Commons licence, and indicate if you modified the licensed material. You do not have permission under this licence to share adapted material derived from this article or parts of it. The images or other third party material in this article are included in the article's Creative Commons licence, unless indicated otherwise in a credit line to the material. If material is not included in the article's Creative Commons licence and your intended use is not permitted by statutory regulation or exceeds the permitted use, you will need to obtain permission directly from the copyright holder. To view a copy of this licence, visit <http://creativecommons.org/licenses/by-nc-nd/4.0/>.

**Keywords** Phospholipid transfer protein (PLTP), Diabetic retinopathy (DR), Vascular dysfunction, DNA methylation, Epigenetics

### Graphical abstract

PLTP promotes the phosphorylation of AKT and GSK3 $\beta$ , leading to the enhancement of endothelial cell proliferation, migration and tube formation, thereby maintaining vascular function. In HG environment, increased DNMT3B expression results in abnormally increased DNA methylation of the PLTP promoter, leading to decreased PLTP expression and subsequent vascular dysfunction.



### Introduction

Diabetic retinopathy (DR), a progressive neurovascular complication of diabetes mellitus (DM), is a leading cause of irreversible visual impairment in middle-aged adults [1]. Microvascular impairment manifests across the spectrum of DR, ranging from initial pathological changes, including microaneurysms and intraretinal hemorrhages in the non-proliferative stage (NPDR), to advanced vascular alterations characterized by capillary non-perfusion and pathological neovascularization in the proliferative stage (PDR) [2, 3]. Nevertheless, effective therapies targeting microvascular pathophysiology of DR remain limited, with a substantial proportion of patients demonstrating suboptimal long-term clinical outcomes [4]. Therefore, a deeper understanding of the vascular injury mechanisms in DR and the identification of novel therapeutic targets are imperative.

Recent advancements in the field of epigenetics have provided novel insights into the pathogenesis and potential treatments for DR [5]. DNA methylation is vital for maintaining genomic stability and regulating gene expression [6]. CpG hypermethylation at gene promoters can induce long-term stable gene silencing by obstructing the binding of transcription factor or chromatin remodeling mediators [7]. Genomic responses to biological, lifestyle, and environmental

factors can alter gene expression patterns through modifications in promoter DNA methylation [8]. Aberrant DNA methylation is involved in DR development, including oxidative stress, inflammation, and neovascularization [9]. We found abnormal DNA methylation of the phospholipid transfer protein (*PLTP*) may be related to DR pathogenesis by utilizing reduced representation bisulfite sequencing (RRBS) and transcriptome sequencing. *PLTP* is essential for endothelial cell function and vascular homeostasis. It has been shown that proper functioning of *PLTP* is crucial for maintaining normal vascular integrity, which be destructed in DR [10]. However, the specific impacts and mechanisms of *PLTP* on vascular dysfunction in DR remain unexplored.

Currently, there are no studies on the epigenetics of *PLTP* in DR. Epigenetic studies of *PLTP* mainly focus on abnormal DNA methylation levels in cardiometabolic diseases [11]. Epigenetic studies in coronary artery disease suggest that alterations in *PLTP* DNA methylation may play an important role in the disease [12]. The methylation level of *PLTP* gene promoter region is significantly correlated with high density lipoprotein cholesterol (HDL-C), low density lipoprotein cholesterol (LDL-C), and triglyceride levels, and may be involved in the pathological process of cardiometabolic diseases

through the lipid metabolic pathway [11, 13]. However, the specific epigenetic mechanisms by which *PLTP* contributes to vascular dysfunction in DR remain unclear.

DNA methyltransferases (DNMTs) and ten-eleven translocation dioxygenases (TETs) play a critical role in DNA methylation. DNMTs transfer methyl groups from S-adenosyl methionine (SAM) to the fifth carbon of cytosine DNA, forming 5-methylcytosine (5mC) and silencing gene transcription [14, 15]. TETs can rapidly hydroxymethylate 5-mC to 5-hydroxymethylcytosine (5-hmC), 5-formylcytosine (5-fC) and 5-carboxylcytosine (5-caC) [16]. This opens the chromatin structure for the binding of transcription factors and promotes the activation and expression of specific genes [17]. DNMTs and TETs are activated in the retina and its vasculature, with their expression varying as diabetes progresses [18]. Additionally, direct inhibition of DNMTs can ameliorate persistent mitochondrial dysfunction and delay DR progression [9]. However, it is not clear which enzyme mediates *PLTP* hypermethylation in DR. This study aims to elucidate the effects of DNA hypermethylation of *PLTP* gene on vascular dysfunction in DR, identify the key enzyme in this process, and clarify the mechanisms by which *PLTP* dysregulation leads to vascular damage in DR. These findings will offer new insights into DR pathogenesis and potential therapeutic targets for vascular injury.

Methods

Diabetic mice

C57BL/6 mice (8 weeks, male) were divided into two groups: control (NC) and DR. To induce the DR model, mice received intraperitoneal injections of streptozotocin (STZ, #S0130, Sigma-Aldrich, USA) in 10 mmol/L citrate

buffer or vehicle (citrate buffer control) for 5 consecutive days. Mice with blood glucose levels above 13.9 mmol/L one week post-injection were considered diabetic mice [19]. Three months after the induction of diabetes, retinal vascular leakage was detected to determine whether there were DR-related changes, including Evans blue (EB) dye leakage and fundus fluorescein angiography.

EB dye leakage

Diabetic and age-matched non-diabetic control mice were injected with 5% EB (100 mg/mL, #E2129, Sigma-Aldrich, USA) via the angular vein. After ensuring systemic circulation of EB by placing the mice on a warm pad at 37 °C for 2 h, eyeballs were collected and fixed in 4% paraformaldehyde for 30 min. Retinas were carefully removed and EB leakage in retinal vessels was observed using confocal microscopy.

Fluorescein fundus angiography (FFA)

Mice were anesthetized via intraperitoneal injection of 1.25% avertin (20 µl/g). Prior to imaging, pupil dilation was achieved using topical application of a 0.5% tropicamide/0.5% phenylephrine mixture. Fluorescein sodium (Alcon Laboratories, USA) was administered intraperitoneally at 5 µl/g body weight [20]. Using a Micron IV Retinal Imaging Microscope (Phoenix Research Labs, USA), imaging begins at 3 min post-injection with brightfield alignment, followed by fluorescence capture at 5, 10, 15, and 20 min (488 nm excitation/520 nm emission).

Table 1 Methylation specific PCR primers

| Gene              | Sequence                        | Product size (bp) | PCR conditions   |
|-------------------|---------------------------------|-------------------|--|
| <i>Pltp</i> -M-F  | 5'-ATTTTGTTAATACGGTGAAATTC-3'   | 178               | 95 °C 5 min;<br>94 °C 20 s,<br>60 °C 30 s,<br>72 °C 20 s,<br>35 cycles;<br>72 °C 5 min |
| <i>Pltp</i> -M-R  | 5'-CCCCCAAATAAATACAATAACG-3'    |                   |  |
| <i>Pltp</i> -U-F  | 5'-TTTGTTAATATGGTGAAATTTGT-3'   | 179               |  |
| <i>Pltp</i> -U-R  | 5'-TCCCCCAAATAAATACAATAACA-3'   |                   |  |
| <i>Prrt1</i> -M-F | 5'-GAAAGAAGGTTTTTTAGGTTTCGT-3'  | 132               |  |
| <i>Prrt1</i> -M-R | 5'-CCCCTTAAAAAATACAAATTCGTA-3'  |                   |  |
| <i>Prrt1</i> -U-F | 5'-TGGAAGAAGGTTTTTTAGGTTTT-3'   | 134               |  |
| <i>Prrt1</i> -U-R | 5'-CCCCTTAAAAAATACAAATTCATA-3'  |                   |  |
| <i>Aen</i> -M-F   | 5'-GTTAGTATGGTCGGTCGTAGTAC-3'   | 113               |  |
| <i>Aen</i> -M-R   | 5'-CAAAACCTCTTCTAATTAATCGAA-3'  |                   |  |
| <i>Aen</i> -U-F   | 5'-GTTAGTATGGTTGGTTGTAGTATGA-3' | 113               |  |
| <i>Aen</i> -U-R   | 5'-CAAAACCTCTTCTAATTAATCAAA-3'  |                   |  |

**Table 2** Real-time PCR primers

| Gene           | Forward primers                  | Reverse primers                  |
|----------------|----------------------------------|----------------------------------|
| Human          |                                  |                                  |
| <i>PLTP</i>    | 5'-GGGCTGCGAGAGGTGATTGAG-3'      | 5'-AATGTGGGAAAAGAGGGGCTGAG-3'    |
| <i>PRRT1</i>   | 5'-CTGTACCATCCTCACCAGTAGTCATC-3' | 5'-GCAGAAAGAGCCTGGGAGATCG-3'     |
| <i>AEN</i>     | 5'-GTGCGGGAGGTGACAACAGAG-3'      | 5'-TGACAGGGAGGGAGCCAGTG-3'       |
| <i>DNMT1</i>   | 5'-GCCTGAGTGTGGAAATGTAAGC-3'     | 5'-CCTCATCGTCATCGCCTCCTTC-3'     |
| <i>DNMT3A</i>  | 5'-GGCTGACAGAGGCACCGTTC-3'       | 5'-CGTGGTCTTTGGAGGCGAGAG-3'      |
| <i>DNMT3B</i>  | 5'-GCAGCCCTGGAGACTCATTGG-3'      | 5'-TTGTTCTCTGGTTCGTGTTTGTG-3'    |
| <i>TET1</i>    | 5'-CTTGCGCAAGTGCTCTCTC-3'        | 5'-GTCACACCAAGTGAAGGCTCAG-3'     |
| <i>TET2</i>    | 5'-TCGAGAGCAGCAGTGAAGAG-3'       | 5'-CCGAGTAGAGTTTGTGAGCCAGAG-3'   |
| <i>TET3</i>    | 5'-CTTCCACTCCAAGTACGCTCTCC-3'    | 5'-AACTGCCACTGTGCCACTG-3'        |
| <i>PI3K</i>    | 5'-AGAGCACTTGGAATCGGAGG-3'       | 5'-CTTCCCCGGCAGTATGCTTC-3'       |
| <i>AKT</i>     | 5'-TGACACCACCGAGCCAAAGATG-3'     | 5'-CAGGAGACACCAGGAAGCACTATG-3'   |
| <i>GSK3β</i>   | 5'-GCACTCTTCAACTTCACCACTCAAG-3'  | 5'-CTGTCCACGGTCTCCAGTATTAGC-3'   |
| <i>β-ACTIN</i> | 5'-GCACCGCAAATGCTTCTA-3'         | 5'-GGTCTTTACGGATGTCAACG-3'       |
| Mouse          |                                  |                                  |
| <i>Pltp</i>    | 5'-AGTGACCTGGACATGCTTCTGAG-3'    | 5'-GATGGAGATGGTGGTGCCTGAC-3'     |
| <i>Prrt1</i>   | 5'-ATCACCACCACCACCATTAC-3'       | 5'-CGGTAGCGTGGCGGAAGAC-3'        |
| <i>Aen</i>     | 5'-GGTTCGGAGAAGACACAAGAGGAG-3'   | 5'-GGTGAAGGCAGAAGGCAGAGAC-3'     |
| <i>Dnmt1</i>   | 5'-CGAGGACAGAGACGAGGATGAG-3'     | 5'-ACGGGAACGGTGTGTGACTC-3'       |
| <i>Dnmt3a</i>  | 5'-AGACCAGAGCAGGCAACAGAC-3'      | 5'-AACGCAAGGTTCTTCCAGGATTG-3'    |
| <i>Dnmt3b</i>  | 5'-AAGACGCACAACCAATGACTCTG-3'    | 5'-GTCTCTCGCTCTCCTCATCCTC-3'     |
| <i>Tet1</i>    | 5'-TGGGCAAGGTTTCAGACTCAC-3'      | 5'-TTGAGAGCTTAGGAAGGAAGATAGG-3'  |
| <i>Tet2</i>    | 5'-AACACTCCAGAGGCACCTTCAG-3'     | 5'-TCCAGAACCAATGAGAACCAACAGAC-3' |
| <i>Tet3</i>    | 5'-CGGCAGGCTGGGAACTTTG-3'        | 5'-TCAGGATGATGGAGAAGGCTACG-3'    |
| <i>Pl3k</i>    | 5'-CGAGAGTGTCTGCACAGTGTG-3'      | 5'-TGTTCTGCTTCCACAACACAG-3'      |
| <i>Akt</i>     | 5'-TGCTGCTCAAGGCGTGATC-3'        | 5'-CGGCTCTGCTTCTCTAAGTCTGAG-3'   |
| <i>Gsk3β</i>   | 5'-GTCACACTGCCGCTCTCCACTC-3'     | 5'-ACATCAGAGCAAGGTATCTCAGAG-3'   |
| <i>β-Actin</i> | 5'-GGCTGTATCCCTCCATCG-3'         | 5'-CCAGTTGGTAACAATGCCATGT-3'     |

**Reduced representation bisulfite sequencing (RRBS), transcriptome sequencing and single-cell sequencing**

Retinal DNA was extracted, qualified, and subjected to bisulfite treatment using the EZ DNA Methylation-gold™ Kit (#D5006, Zymo Research, USA), followed by PCR amplification to obtain the final DNA library. Sequencing results were reverse-complemented and aligned with the reference genome. Differentially methylated genes (DMGs) were identified through statistical analysis. Concurrently, transcriptome analyses quantified gene expression, identifying differentially expressed genes (DEGs). Intersection of DMG and DEG datasets revealed aberrantly methylated genes in DR, including hypermethylated down-regulated and hypomethylated up-regulated genes. Details of single-cell sequencing are provided in our previous studies [21]. Raw single-cell data generated by Illumina platforms were pre-processed using Cell Ranger to obtain gene expression matrices. These matrices were imported into Seurat for analysis, with batch effect correction performed

via Harmony. Elbow Plot identified 30 principal components as optimal, followed by dimensionality reduction visualization using RunTSNE and RunUMAP. Cells were clustered via Find Neighbors and classified into homogeneous groups with Find Cluster, yielding final clustering results. Marker genes for distinct subpopulations were identified using Find All Markers, enabling cell type annotation based on marker gene signatures.

**Cell culture, transfection and inhibitor treatments**

Consistent with single-cell RNA sequencing and immunofluorescence staining results, human retinal microvascular endothelial cells (HRMECs) were selected as the cell model. HRMECs were obtained from Applied Cell Biology Research Institute (#ACBRI 181; Kirkland, USA) and cultured as described in the supplementary

document [22]. Cells were treated with different concentrations (5  $\mu$ M, 10  $\mu$ M, 20  $\mu$ M) of GSK3 $\beta$  inhibitor (#BRD3731, MedChemExpress, USA) for 48 h.

The *PLTP* expression plasmid (OE-*PLTP*, pcDNA3.1-*PLTP*) was purchased from Hanbio (Shanghai, China) and transfected using Lipofectamine™ 3000 (#L3000008, Thermo Fisher Scientific, USA). Small interfering RNAs targeting *PLTP* (si*PLTP*), *DNMT1* (si*DNMT1*), *DNMT3B* (si*DNMT3B*) and negative control (siNC) were purchased from RiboBio (Guangzhou, China), and transfected using Lipofectamine® RNAiMAX transfection reagent (#13,778,075, Thermo Fisher Scientific, USA).

#### DNA extraction, bisulfite conversion, and methylation-specific PCR (MS-PCR)

Procedures and reagents were as described in the supplementary document. The intensity of methylated to unmethylated bands (M/U) was analyzed and quantified. Primers were obtained from Sangon Biotech (Shanghai, China) and are listed in Table 1.

#### RNA extraction and real-time PCR

Procedures and reagents were as described in the supplementary document. Specific primers were obtained from Sangon Biotech (Shanghai, China) and are listed in Table 2.  $\beta$ -Actin served as the housekeeping gene.

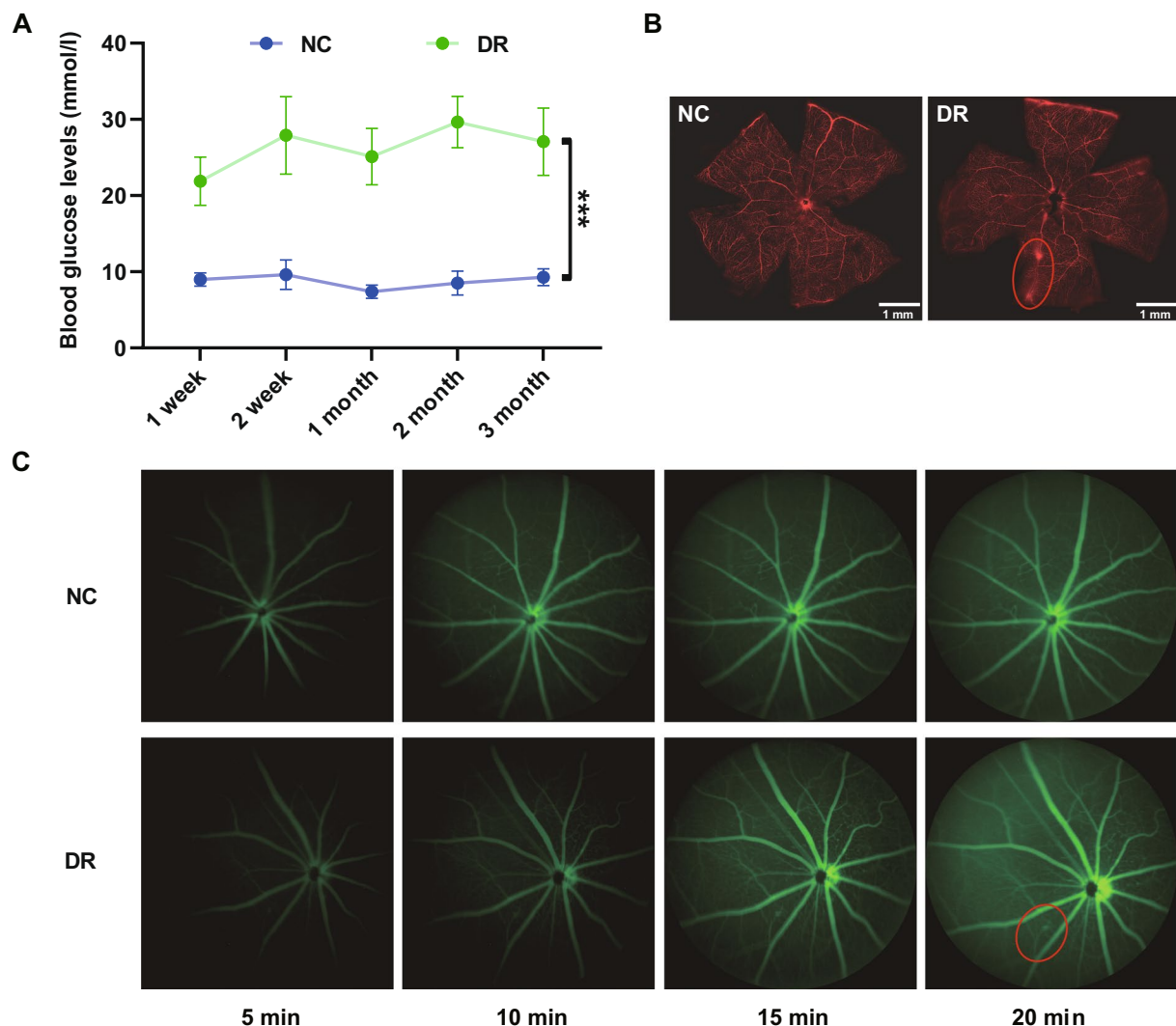


**Fig. 1** Induction of a DR Mouse Model and Identification of Diabetic Retinopathy. **A** Blood glucose levels in mice after the last injection (NC vs DM mice,  $n=40$ ). **B** Evans blue dye leakage in the retinas (NC and DR mice,  $n=3$ ). **C** Fluorescein fundus angiography of the retinas (NC and DR mice,  $n=3$ ). NC, normal control; DR, diabetic retinopathy. \*\*\* $p < 0.001$

### Protein extraction and western blotting (WB)

Proteins extracted from HRMECs were separated by 4–20% SDS-PAGE (#M00930, GenScript, USA) and transferred onto polyvinylidene fluoride membranes (#IPVH00010, Millipore, Ireland). After blocking with 5% nonfat milk or bovine serum albumin (BSA, #4240, BioFroxx, Germany) for 2 h, membranes were incubated with primary antibodies against PLTP (1:1500, #PA5-102,820, Thermo Fisher Scientific, USA), DNMT1 (1:1000, #ab188453, Abcam, UK), DNMT3A (1:1000, #ab307503, Abcam, UK), DNMT3B (1:1000, #PA5-91,864, Thermo Fisher Scientific, USA), PI3K (1:1000, #4249 T, Cell Signaling Technology, USA), AKT (1:1000, #4685S, Cell Signaling Technology, USA), phosphorylated AKT (p-AKT, 1:1000, #4060 T, Cell Signaling Technology, USA), GSK3 $\beta$  (1:4000, #22,104–1-AP, Proteintech, China), phosphorylated GSK3 $\beta$  (p-GSK3 $\beta$ , 1:1000, #29,125–1-AP, Proteintech, China), VEGFR1 (1:3000, #ab32152, Abcam, UK) or VEGFR2 (1:1000, #ab39638, Abcam, UK). Secondary antibodies (1:50,000, #98,261 and #97,910, Jackson ImmunoResearch, USA) were used.  $\beta$ -ACTIN (1:30,000, #66,009–1-Ig, Proteintech, China) served as standard controls. ImageJ software was employed to analyze the ratio of phosphorylated AKT to AKT (p-AKT/AKT) or phosphorylated GSK3 $\beta$  to GSK3 $\beta$  (p-GSK3 $\beta$ /GSK3 $\beta$ ).

### Cell migration and tube formation assays

**Cell Migration:** A total of  $5 \times 10^4$  cells from each group were seeded in 200  $\mu$ l serum-free medium and observed after 16–18 h of migration. **Tube Formation:** HRMECs were seeded at 8000 cells per well in 50  $\mu$ l of complete medium and at 37 °C for 3–4 h. Specific procedures and reagents were as described in the supplementary document. Migrating cells and tubular networks were imaged and quantified by ImageJ software.

### Enzyme-linked immunosorbent assay (ELISA)

The level of IL-1 $\beta$  (ab214025, Abcam, UK) and IL-18 (ab215539, Abcam, UK) protein was determined using

a colorimetric ELISA kit according to the manufacturer's instructions.

### Luciferase reporter assay

The *PLTP* promoter was constructed upstream of the firefly luciferase (FLuc) in the pGL3-basic vector, and *DNMT3B* was constructed into the pcDNA3.1 vector with renilla luciferase (Rluc). Co-transfection into cells was followed by luciferase activity measurement to analyze FLuc/Rluc activity in response to *PLTP* promoter activity.

### RNA extraction, library construction, illumina sequencing (RNA-Seq), and data analysis

Total RNA was extracted from HRMECs using TRIzol reagent (#15596018CN, Invitrogen, USA). Differential expression analysis of the two groups was performed using the DESeq2 R package. Transcripts with a fold change > 2 or < -2 and an adjusted *p* value < 0.05 were considered differentially expressed genes. Gene Ontology (GO) and Kyoto Encyclopedia of Genes and Genomes (KEGG) pathway enrichment analyses were conducted by the clusterProfiler R package. GO terms and KEGG pathways with *p* < 0.05 were considered significantly enriched.

### Coimmunoprecipitation (co-IP)

Co-IP assays were performed to investigate interactions between PLTP and AKT or GSK3 $\beta$ . Co-IP was conducted using the Pierce CO-IP Kit (#26,149, Thermo Fisher Scientific, USA). Cells were lysed in IP lysis buffer containing a protease/phosphatase inhibitor cocktail. The anti-PLTP antibody was immobilized with AminoLink Plus coupling resin or control resin at room temperature for two hours. The cell lysates were incubated overnight at 4 °C, with agarose resin conjugated to the anti-PLTP antibody and with control agarose resin not bound to PLTP. Western blotting was used to analyze the eluted immunoprecipitated samples after washing.

(See figure on next page.)

**Fig. 2** Abnormal DNA Hypermethylation of *Pltp* Promoter is Associated with DR. **A** Venn diagram of the DMG and DEG. **B** Expression of three key genes (*Pltp*, *Prmt1*, and *Aen*) with abnormal DNA methylation in the retina (NC vs DR mice, *n* = 3). **C** Agarose gel electrophoresis results of MS-PCR products of the key genes and quantitative analysis of promoter methylation levels (NC vs DR mice, *n* = 5). **D** Western blot analysis of PLTP in retina (NC vs DR mice, *n* = 3). **E** Single-cell sequencing showing *Pltp* predominantly distributed in retinal cells ((NC vs DR mice, *n* = 3). **F** Retinas from mice with diabetic retinopathy and non-diabetic controls were incubated with antibodies against PLTP and vWF, followed by secondary antibodies conjugated with Alexa Fluor 488 and Alexa Fluor 647 respectively (NC vs DR mice, *n* = 3). Red boxes show areas that co-express vWF and PLTP which surround retinal endothelial cells. DMG, differentially methylated genes; DEG, differentially expressed genes; MS-PCR, methylation-specific PCR; M, methylation bands; U, unmethylated bands; M/U, quantifying the ratio of the intensity of the methylated band to the unmethylated band; NC, normal control; DR, diabetic retinopathy; vWF, von Willebrand factor. \**p* < 0.05, \*\**p* < 0.01, \*\*\**p* < 0.001



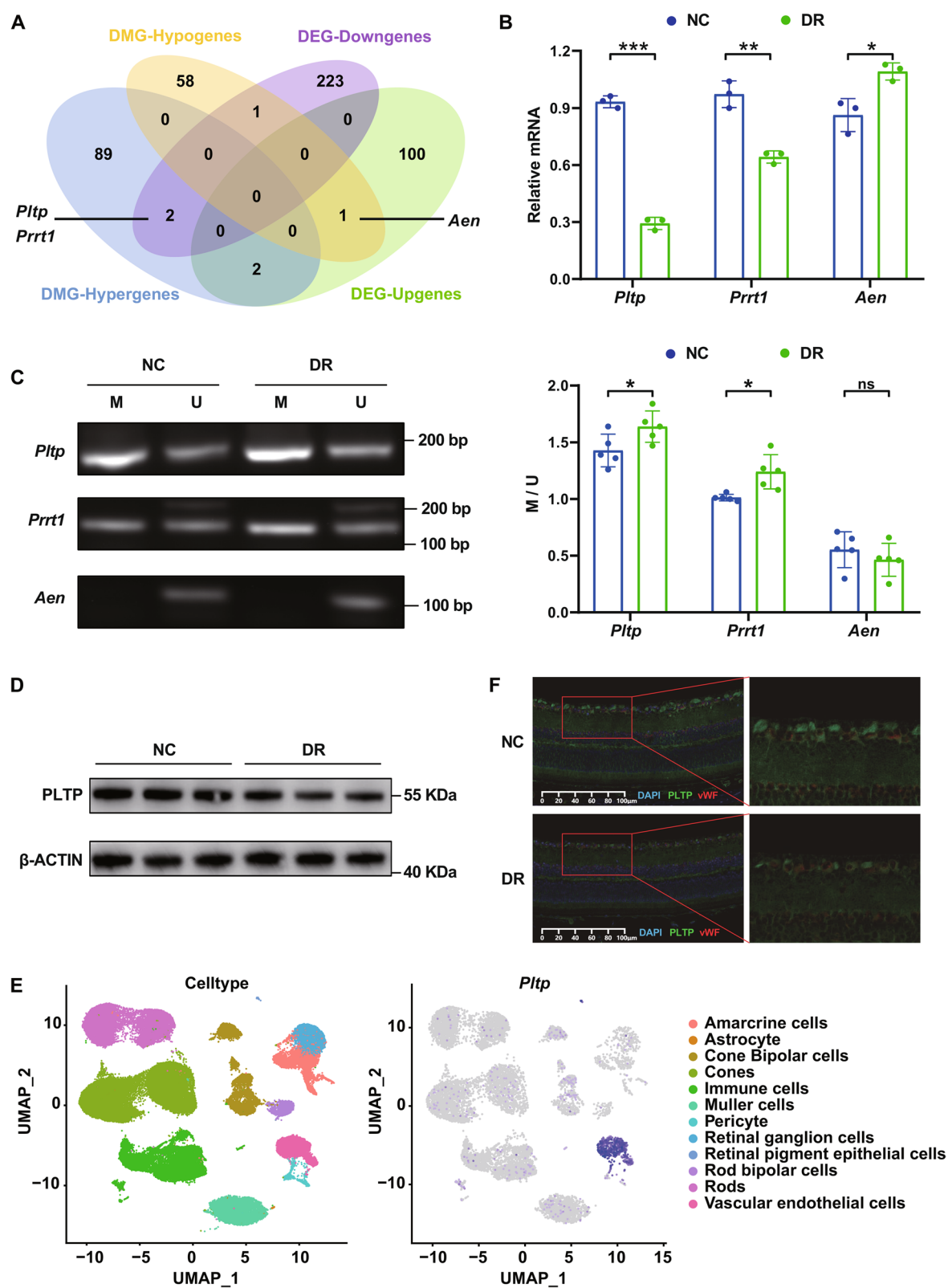


**Fig. 2** (See legend on previous page.)

### Immunofluorescence staining

Retinas from DR mice and non-diabetic controls were fixed for 10 min at  $-20^{\circ}\text{C}$  and incubated with antibodies against von Willebrand factor (vWF; endothelial cell marker) and PLTP, followed by secondary antibodies conjugated with Alexa Fluor 488 (#ab150117, Abcam, UK) and Alexa Fluor 647 (#ab150075, Abcam, UK) respectively. Arrowheads show areas that co-express vWF and PLTP which surround retinal endothelial cells. Nuclei were stained with 4',6-diamidino-2-phenylindole (DAPI).

### Statistical analysis

Data are presented as means  $\pm$  standard deviations. Differences between groups were analyzed using 2-tailed Student's *t*-test by GraphPad Prism (ver. 8.0; San Diego, USA) and SPSS (ver. 26.0; Chicago, USA). Notably,  $p < 0.05$  was considered statistically significant.

## Result

### Increased DNA methylation in *Pltp* promoter is associated with DR

STZ-induced diabetic mouse models were successfully generated (Fig. 1A). EB leakage and FFA results confirmed the presence of retinal vascular leakage in DM mice, indicating successful DR model construction. Leakage or microaneurysm areas are highlighted by red circles (Fig. 1B–C). Combined analysis of RRBS and transcriptome sequencing of DR and NC mice retinas revealed differences in genomic methylation levels, with hypermethylated down-regulated genes and hypomethylated up-regulated genes (Fig. S1A, B). Three key genes with abnormal DNA methylation were screened out, including *Pltp*, proline-rich transmembrane protein 1 (*Prprt1*) and apoptosis-enhancing nuclease (*Aen*) (Fig. 2A). The retina tissue was used to verify the DNA methylation and mRNA expression levels of these genes. Real-time PCR results revealed decreased *Pltp* and *Prprt1* mRNA expression, concurrent with increased *Aen* expression (Fig. 2B). MS-PCR analysis demonstrated elevated methylation levels in the promoter regions of *Pltp* and *Prprt1* genes, whereas *Aen* methylation remained unchanged (Fig. 2C). The inverse correlation between hypermethylation and reduced mRNA levels for *Pltp* and *Prprt1* aligned with the established epigenetic principle that

DNA hypermethylation silences gene transcription, with *Pltp* exhibiting a more pronounced expression discrepancy compared to *Prprt1*. Protein expression validation indicated decreased PLTP levels in DR mouse retinas (Fig. 2D). Therefore, increased DNA methylation of *Pltp* promoter correlates with decreased mRNA and protein expression in DR mouse retinas.

### PLTP regulates the function of vascular endothelial cells

The results of retinal single-cell sequencing analysis showed that *Pltp* was mainly expressed in vascular endothelial cells (Fig. 2E). This was also confirmed by immunofluorescence and PLTP fluorescence appeared to be reduced in the DR group compared with the NC group (Fig. S1C and Fig. 2F). Therefore, we established an in vitro endothelial cell model to explore the expression and functional mechanisms of PLTP in DR. MS-PCR results suggested that DNA methylation of *PLTP* promoter was increased in HRMECs treated with HG (Fig. 3A). Subsequently, the results of PCR and WB suggested that mRNA and protein expression were also significantly decreased in HRMECs treated with HG (Fig. 3B, C). Next, this study used cell migration and tube formation assays to further examine the role of PLTP in the function of vascular endothelial cells. The results showed that *PLTP* knockdown and HG incubation enhanced the migration and tube formation ability of endothelial cells, while *PLTP* overexpression reversed HG-induced effects on endothelial cells (Fig. 3D–H). ELISA assays display an elevation of IL-1 $\beta$  and IL-18 in HRMECs treated by *PLTP* knockdown or high glucose, and this trend can be reversed by *PLTP* overexpression (Fig. 3I).

### DNMT3B is a key enzyme in aberrant *PLTP* methylation

PCR analysis of mouse retinas and HG-treated HRMECs revealed that DNMTs and TETs were generally increased in the DR group. Among them, *DNMT1* and *DNMT3B* demonstrated a more stable trend and a more significant change than other enzymes in HRMECs and retina (Fig. 4A, B). The DNA methylation level of *PLTP* is increased in DR, and it is closely related to DNMTs. Therefore, further study focused on exploring the effect of DNMTs (especially DNMT1 and DNMT3B) on the methylation of *PLTP* promoter. The protein expression

(See figure on next page.)

**Fig. 3** Abnormal PLTP is Involved in Vascular Dysfunction in DR. **A** Agarose gel electrophoresis results of MS-PCR products of *PLTP* in HRMECs and quantitative analysis of promoter methylation levels (NC vs HG,  $n=3$ ). **B** *PLTP* expression in HRMECs (NC vs HG,  $n=3$ ). **C** Western blot and quantitative analysis of PLTP in HRMECs (NC vs HG,  $n=3$ ). Migration assay of HRMECs **D** and quantitative analysis **E** (NC, NC + siPLTP, HG and HG + OE-PLTP,  $n=5$ ). Tube formation assay of HRMECs **F**, and quantitative analysis of nodes **G** and branches length **H** (NC, NC + siPLTP, HG and HG + OE-PLTP,  $n=3$ ). **I** ELISA results of IL-1 $\beta$  and IL-18 in HRMECs (NC, NC + siPLTP, HG and HG + OE-PLTP,  $n=3$ ). MS-PCR, methylation-specific PCR; M, methylation bands; U, unmethylated bands; M/U, quantifying the ratio of the intensity of the methylated band to the unmethylated band; NC, normal control; HG, high glucose. \* $p < 0.05$ , \*\* $p < 0.01$ , \*\*\* $p < 0.001$



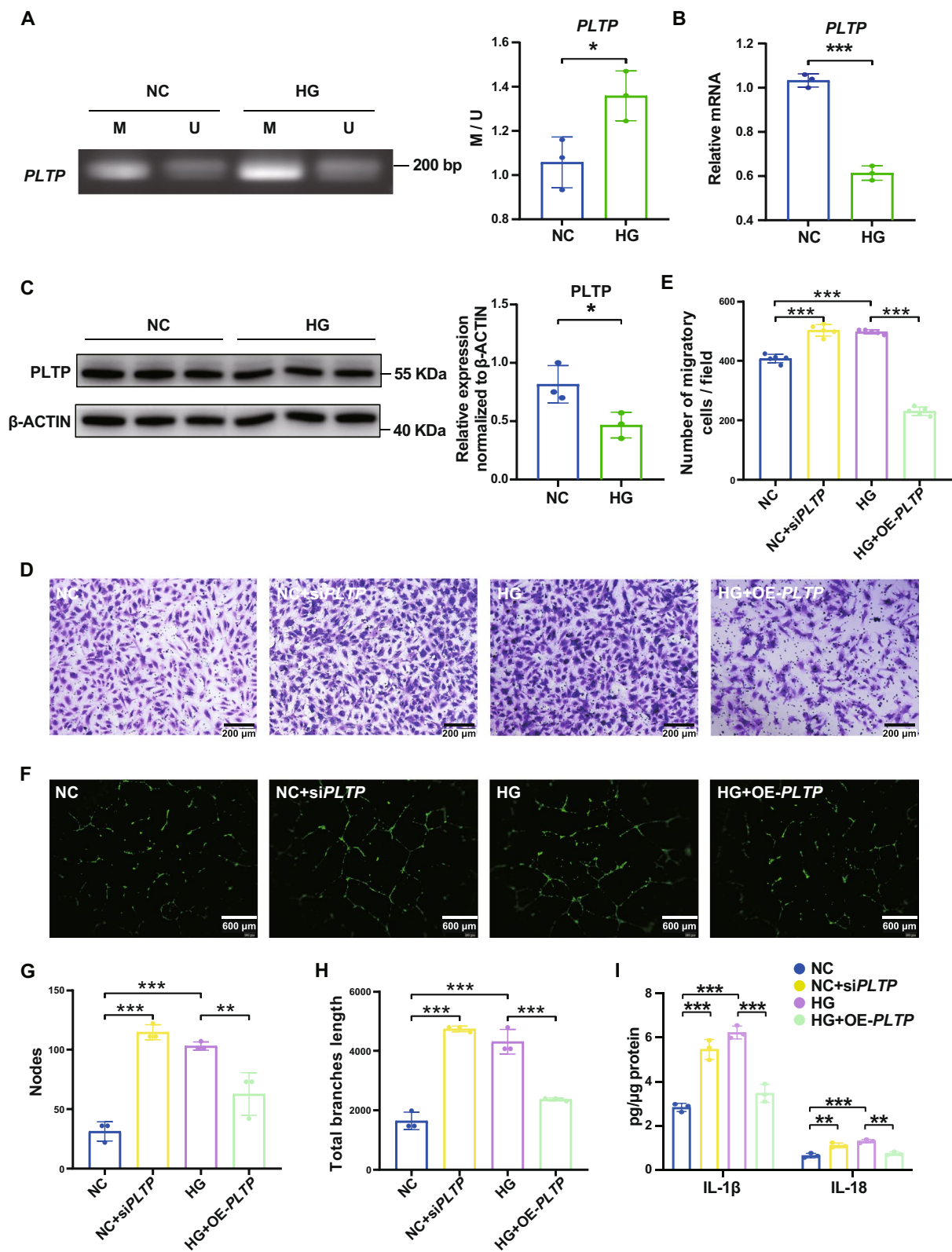


**Fig. 3** (See legend on previous page.)

of DNMT1 and DNMT3B was increased in the retinas of DR mice and HRMECs incubated with HG (Fig. 4C). There was no significant change in the expression of DNMT3A (Fig. S2A, B). We identified siRNAs with the highest efficiency, including siDNMT1#3 and siDNMT3B#1 (Fig. S2C). By constructing DNMT1- and DNMT3B-knockdown cell models, the results of MS-PCR, real-time PCR, and WB showed that DNMT3B knockdown significantly reduced the DNA methylation of *PLTP* promoter, and the mRNA and protein expressions were significantly increased (Fig. 4D–F and Fig. S2C). Luciferase reporter assay was further used to determine the binding of DNMT3B to the *PLTP* promoter, and the results showed that DNMT3B interacted with the *PLTP* promoter (Fig. 4G). Besides, DNMT3B knockdown reversed the enhanced migration and tube formation ability of endothelial cells induced by HG (Fig. 4H–K). This suggested that DNMT3B may be the key enzyme responsible for the abnormal DNA methylation of the *PLTP* promoter in DR.

#### AKT/GSK3 $\beta$ is the key downstream pathway of PLTP

After constructing the *PLTP*-knockdown cell model, the cells were collected for transcriptome sequencing and functional analysis was used to screen out the related pathways of PLTP, among which PI3K/AKT/GSK3 $\beta$  signaling pathway was the most significant (Fig. 5A and Fig. S3A). Consistent with PLTP, PI3K/AKT/GSK3 $\beta$  also plays a role in regulating vascular function, so this pathway was selected for subsequent studies. Based on the significant finding of the PI3K/AKT/GSK3 $\beta$  signaling pathway from the above analysis, Co-IP was then used to explore the relationship between PLTP and PI3K/AKT/GSK3 $\beta$ , indicating the interactions between PLTP and AKT or GSK3 $\beta$  (Fig. 5B). Given that phosphorylated AKT and phosphorylated GSK3 $\beta$  are the active forms of the PI3K/AKT/GSK3 $\beta$  signaling pathway, we subsequently studied the ratio of the phosphorylated form to the unphosphorylated form to show the relative activities. The levels of p-AKT/AKT and p-GSK3 $\beta$ /GSK3 $\beta$  measured by WB analysis were decreased in *PLTP* knockdown and HG treatment groups, while *PLTP* overexpression reversed the decrease of p-AKT/AKT

and p-GSK3 $\beta$ /GSK3 $\beta$  induced by HG (Fig. 5C, D). Similar results were observed in mouse models. In the DR group, p-AKT/AKT and p-GSK3 $\beta$ /GSK3 $\beta$  levels were decreased (Fig. 5E, F). PCR demonstrated similar results. In HRMECs, *GSK3 $\beta$*  and *AKT* expression decreased in HG and *PLTP* knockdown groups, while *PLTP* overexpression reversed HG-induced decrease in *GSK3 $\beta$*  and *AKT* expression. In the retina, the expression of *Gsk3 $\beta$*  and *Akt* also decreased in DR (Fig. S3B, C).

#### Anti-angiogenic properties of PLTP depend on AKT/GSK3 $\beta$ pathway

To investigate the correlation between PLTP and AKT/GSK3 $\beta$  in regulating vascular dysfunction, HRMECs were treated with a selective GSK3 $\beta$  inhibitor (BRD3731). Results showed that the level of pGSK3 $\beta$ /GSK3 $\beta$  was significantly decreased after BRD3731 treatment (Fig. 6A, B). This means that inhibition of GSK3 $\beta$  could reverse the increase of p-GSK3 $\beta$ /GSK3 $\beta$  level induced by *PLTP* overexpression. Inhibition of GSK3 $\beta$  reversed the enhanced migration and tube formation ability of endothelial cells induced by *PLTP* overexpression (Fig. 6C–G). In addition, VEGFR1 and VEGFR2 were selected as markers of endothelial cell proliferation. It was found that the expression of VEGFR1 and VEGFR2 was increased in HG and *PLTP* knockdown groups, and *PLTP* overexpression reversed the increased expression of VEGFR1 and VEGFR2 induced by HG treatment (Fig. S4B). The expression of VEGFR1 and VEGFR2 was also increased in retina of DR mice (Fig. S4C). GSK3 $\beta$  inhibition could reverse the effect of *PLTP* overexpression on VEGFR1 or VEGFR2 expression (Fig. 6A and Fig. S4A). These results indicate that the anti-vascular dysfunction effect of PLTP may be related to its regulation on AKT/GSK3 $\beta$  pathway.

#### Discussion

This study is the first to investigate the role of PLTP in DR, focusing on aberrant methylation of the *PLTP* gene and identifying the key enzymes involved. Additionally, the role of Akt/GSK3 $\beta$  signaling pathway in retinal vascular endothelial cell function, in conjunction with PLTP, was explored to understand its impact on vascular dysfunction in DR.

(See figure on next page.)

**Fig. 4** DNMT3B is the Main Enzyme Affecting the Abnormal Methylation of the *PLTP* Promoter. **A** Expression of enzymes involved in DNA methylation in HRMECs (NC vs HG, n=8). **B** Expression of enzymes involved in DNA methylation in retina (NC vs DR mice, n=3). **C** Western blot analysis of DNMT1 and DNMT3B in HRMECs (NC vs HG, n=3) or retina (NC vs DR mice, n=3). **D** Quantitative analysis of promoter methylation levels of *PLTP* in HRMECs (siNC, siDNMT1 and siDNMT3B, n=3). **E** PCR analysis of *PLTP* in HRMECs (siNC, siDNMT1 and siDNMT3B, n=3). **F** Western blot analysis of PLTP in HRMECs (siNC, siDNMT1 and siDNMT3B, n=3). **G** Luciferase reporter assay for DNMT3B interaction with the *PLTP* promoter (n=3). Migration assay of HRMECs **H** and quantitative analysis **I** (HG vs HG + siDNMT3B, n=5). Tube formation assay of HRMECs **J**, and quantitative analysis of nodes and branches length **K** (HG vs HG + siDNMT3B, n=3). NC, normal control; HG, high glucose; DR, diabetic retinopathy; FLuc, firefly luciferase; RLuc, renilla luciferase. \* $p < 0.05$ , \*\* $p < 0.01$ , \*\*\* $p < 0.001$

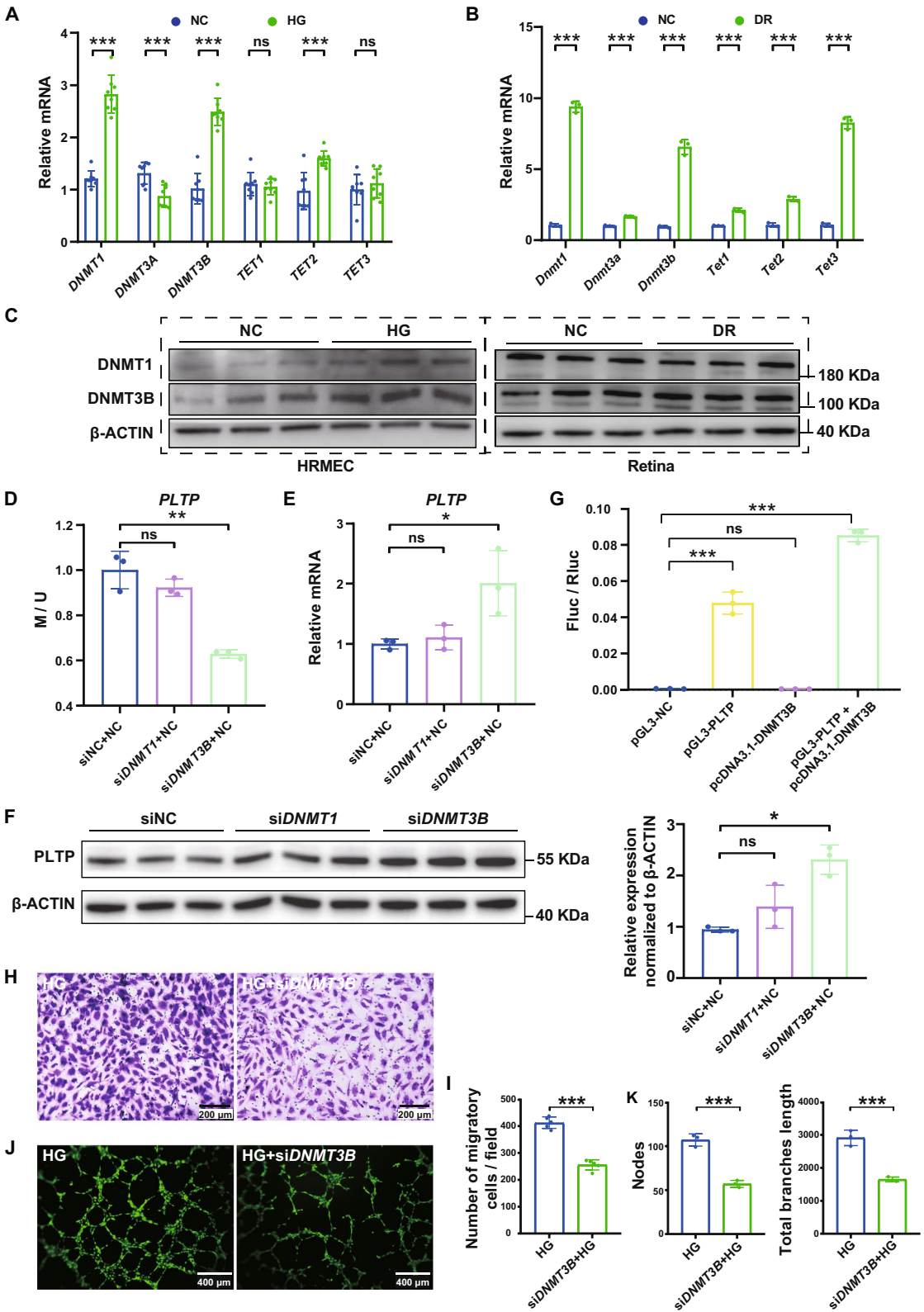


**Fig. 4** (See legend on previous page.)

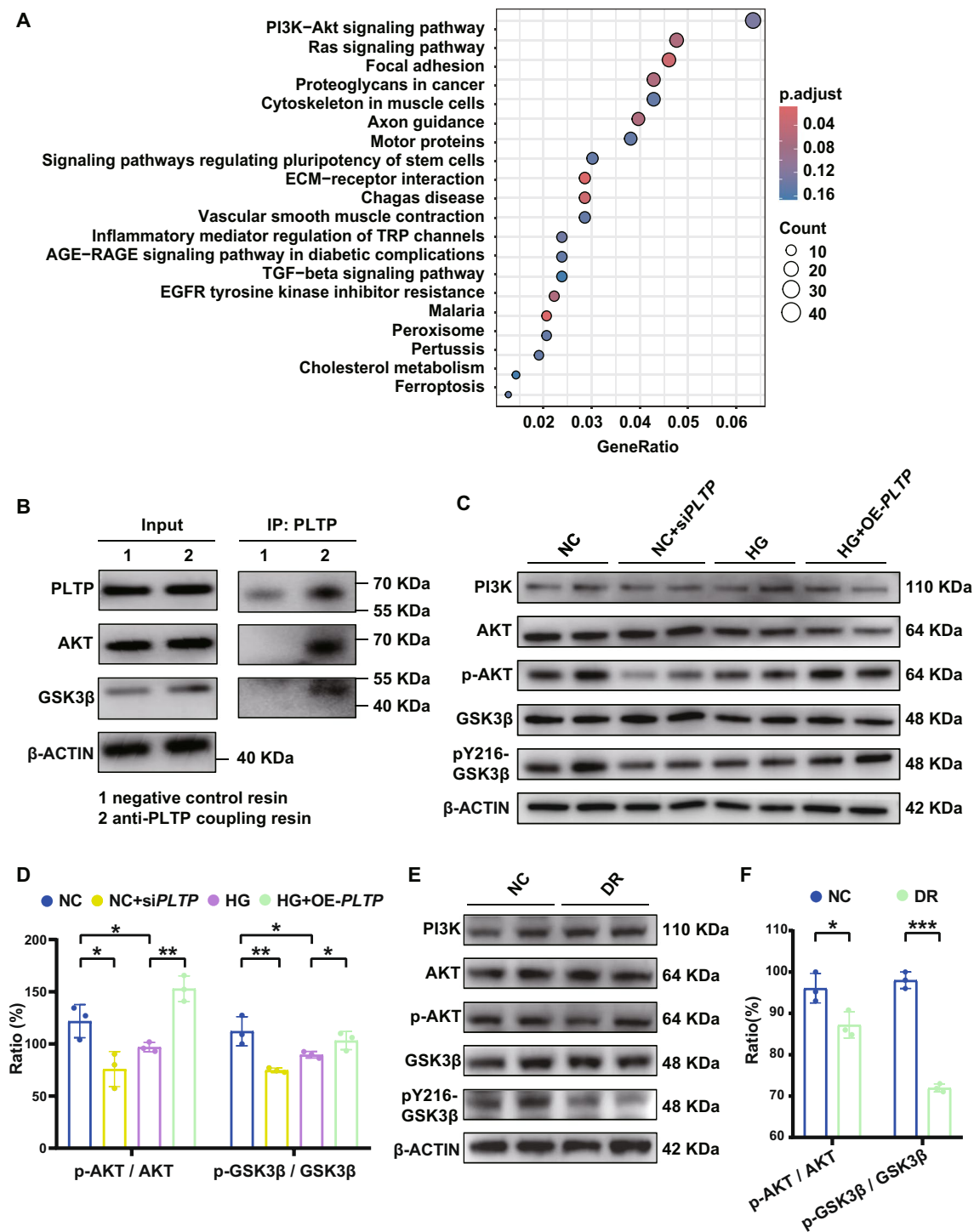


**Fig. 5** AKT/GSK3β is the Key Downstream Pathway of PLTP Gene. **A** KEGG enrichment analysis of differentially expressed genes after *PLTP* knockdown (NC vs siPLTP, n = 3). **B** Co-IP assays of PLTP interaction with AKT or GSK3β. Western blot analysis of PI3K/AKT/GSK3β **C** and quantitative analysis of p-AKT/AKT or p-GSK3β/GSK3β **D** in HRMECs (NC, NC + siPLTP, HG and HG + OE-PLTP, n = 3). Western blot analysis of PI3K/AKT/GSK3β **E** and quantitative analysis of p-AKT/AKT or p-GSK3β/GSK3β **F** in retina (NC vs DR mice, n = 3). KEGG, Kyoto Encyclopedia of Genes and Genomes; NC, normal control; HG, high glucose; DR, diabetic retinopathy. \**p* < 0.05, \*\**p* < 0.01, \*\*\**p* < 0.001



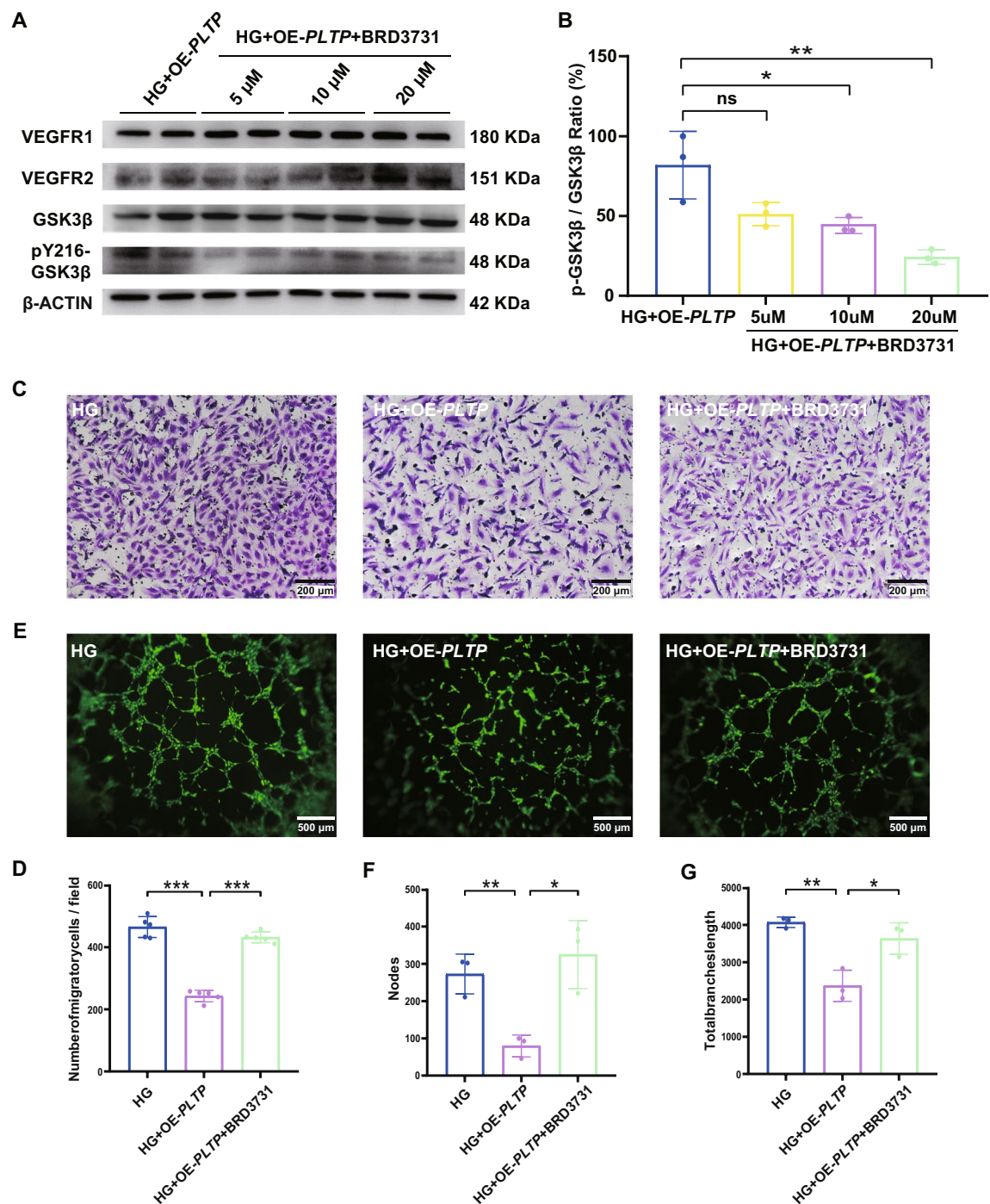


**Fig. 6** The anti-angiogenic properties of PLTP depend on PI3K/AKT/GSK3β pathway. Western blot analysis **A** and quantitative analysis of p-GSK3β/GSK3β **B** in HRMECs (HG + OE-PLTP vs HG + OE-PLTP + BRD3731, n = 3). Migration assay of HRMECs **C** and quantitative analysis **D** (HG, HG + OE-PLTP and HG + OE-PLTP + BRD3731, n = 5). Tube formation assay of HRMECs **E**, and quantitative analysis of nodes **F** and branches length **G** (HG, HG + OE-PLTP and HG + OE-PLTP + BRD3731, n = 3). HG, high glucose. \*p < 0.05, \*\*p < 0.01, \*\*\*p < 0.001

DNA methylation plays a crucial role in both normal and pathological development of the human retina [23]. In normal cells, DNA methylation ensures the temporal

and spatial accuracy of gene expression, essential for mammalian development [24]. For instance, it has been shown to maintain specific gene expression patterns

in retinal cells (photoreceptor and non-photoreceptor cells) [25, 26]. Aberrant DNA methylation is implicated in retinal diseases. Certain genes with abnormal DNA methylation contribute to neovascularization, promoting DR development [27]. Overexpression of maternally expressed gene 3 (*MEG3*) can reduce pathological expression of vascular endothelial growth factor (VEGF), inhibit endothelial-mesenchymal transition, and block DR development [27, 28]. However, *MEG3* expression is significantly reduced in DR, due to aberrant regulation on DNA methylation induced by DNMTs [27]. In addition, CpG methylation has been shown to regulate angiogenic pathways such as *ETS1*, *HES5* and *PRDM16* in DR progression [29].

Our study discovered that abnormal DNA methylation of *PLTP* gene is associated with DR pathogenesis. PLTP is a phospholipid transfer protein crucial for lipid metabolism and transport [30]. PLTP facilitates the formation and remodeling of high-density lipoprotein (HDL) particles through the accumulation and transport of phospholipids, vitamin E and free cholesterol, playing an important role in the development of atherosclerosis and cardiometabolic diseases [31, 32]. Studies in retinopathy have shown that PLTP is vital for retinal lipoprotein metabolism, and its dysregulation may lead to the accumulation of subretinal lipids, ultimately leading to age-related macular degeneration (AMD) [33, 34]. Studies in vascular function have shown that PLTP plays an important role in maintaining endothelial cell function and vascular homeostasis by regulating the distribution of vitamin E and its metabolite  $\alpha$ -tocopherol in vascular tissues, especially in the vascular wall [10]. Our findings further confirmed that PLTP expression regulates the proliferation, tube formation, and migration ability of vascular endothelial cells, significantly influencing vascular dysfunction in DR.

The PI3K/AKT/GSK3 $\beta$  signaling pathway is extensively studied, and PI3K induces AKT phosphorylation, playing a key role in cellular response to extracellular signals, regulation of cell survival and angiogenesis [35]. GSK3 $\beta$ , a downstream factor in the PI3K/AKT signaling pathway, is phosphorylated by phosphorylated AKT [35]. High glucose levels decrease activated AKT in tissues such as the liver and retina, leading to abnormal GSK3 $\beta$  activity [36]. Previous studies have linked aberrant DNA methylation to the PI3K/AKT/GSK3 $\beta$  pathway in various pathological conditions [37]. For example, abnormal DNA methylation leads to the abnormal expression of tumor endothelial marker 8 (*TEM8*), enhancing cell proliferation, invasion, migration, drug resistance, radiation resistance and the recurrence of glioblastoma [38]. These effects are primarily mediated through the AKT/GSK3 $\beta$  pathway [38]. Our study enriches this understanding by elucidating the role of aberrantly methylated PLTP in regulating the AKT/GSK3 $\beta$  pathway in DR. The regulation

of this pathway is crucial for reducing pericyte apoptosis, resisting epithelial-mesenchymal transition, and managing oxidation–reduction progress, ultimately improving DR and other proliferative retinopathy [39–41]. Our findings suggest that PLTP overexpression may ameliorate endothelial dysfunction and improve DR via the AKT/GSK3 $\beta$  pathway, highlighting its key role in DR vascular dysfunction.

Modulating DNA methylation patterns or developing specific inhibitors targeting PLTP or the AKT/GSK3 $\beta$  pathway could offer potential therapeutic strategies for DR. DNA methylation modifiers such as DNMTs inhibitors or demethylating agents, could restore normal methylation patterns and alleviate vascular dysfunction in DR [9, 42]. It has been shown that abnormalities in retinal DNA methylation-hydroxymethylation progress do not immediately improve with glycemic control. However, direct inhibition of DNMTs can ameliorate abnormal DNA methylation, mitigating persistent mitochondrial dysfunction and delaying DR development [43]. DNMTs inhibitor, such as 5-aza-2'-deoxycytidine, can reverse increased DNMTs levels and maintain oxidation–reduction homeostasis by regulating antioxidant enzymes, demonstrating promising therapeutic potential for DR [44].

The neurovascular unit damage underlying DR pathogenesis manifests through multifaceted pathological processes, including pericyte depletion, endothelial dysfunction, neurodegeneration, and chronic inflammation [45]. Emerging evidence indicates these pathological cascades are driven by complex intercellular crosstalk within the neurovascular microenvironment [46]. Accumulating evidence demonstrates that activated endothelial cells drive neurovascular crosstalk dysregulation through pro-inflammatory cytokine secretion and blood-retinal barrier disruption [45–47]. Our study revealed that PLTP suppresses endothelial inflammatory mediator production, suggesting its potential to modulate neuronal function through cytokine-dependent mechanisms. Nevertheless, rigorous mechanistic investigations are warranted to delineate the precise regulatory role of PLTP in DR-associated neurovascular pathophysiology.

Despite the insights provided, our study has certain limitations. It primarily focused on the association between abnormal PLTP expression and vascular dysfunction in DR, with only preliminary exploration of the mechanisms underlying abnormal DNA methylation of the *PLTP* promoter. While DNMT3B was identified as a key enzyme in *PLTP* gene methylation, the specific mechanism of DNMT3B-induced methylation was not verified. This study did not include DNMT3B inhibition experiments to verify the therapeutic effects of selective DNMTs inhibitors on DR, which is a limitation that future research should address.



## Conclusion

In conclusion, this study is the first to explore the potential role of DNA hypermethylation of *PLTP* in vascular dysfunction, providing new insights into the pathogenesis of DR. Under high glucose conditions, *PLTP* upregulation mediated by DNMT3B-induced DNA hypermethylation exacerbates vascular dysfunction in DR through the AKT/GSK3 $\beta$  signaling pathway. These findings are expected to open novel avenues for understanding DR pathology and developing targeted therapeutic strategies.

## Abbreviations

|        |   |
|--------|---|
| DR     | Diabetic retinopathy                          |
| DM     | Diabetes mellitus                             |
| NPDR   | Non-proliferative diabetic retinopathy        |
| PDR    | Proliferative diabetic retinopathy            |
| PLTP   | Phospholipid transfer protein                 |
| HDL-C  | High density lipoprotein cholesterol          |
| LDL-C  | Low density lipoprotein cholesterol           |
| DNMTs  | DNA methyltransferases                        |
| TETs   | Ten-eleven translocation dioxygenases         |
| SAM    | S-adenosyl methionine                         |
| 5mC    | 5-Methylcytosine                              |
| EB     | Evans blue                                    |
| FFA    | Fluorescein fundus angiography                |
| DMG    | Differentially methylated genes               |
| DEG    | Differentially expressed genes                |
| HRMECs | Human retinal microvascular endothelial cells |
| MS-PCR | Methylation-specific PCR                      |
| WB     | Western blotting                              |
| ELISA  | Enzyme-linked immunosorbent assay             |
| FLuc   | Firefly luciferase                            |
| Rluc   | Renilla luciferase                            |
| GO     | Gene ontology                                 |
| KEGG   | Kyoto encyclopedia of genes and genomes       |
| vWF    | Von Willebrand factor                         |
| PRRT1  | Proline-rich transmembrane protein 1          |
| AEN    | Apoptosis-enhancing nuclease                  |
| MEG3   | Maternally expressed gene 3                   |
| VEGF   | Vascular endothelial growth factor            |
| HDL    | High-density lipoprotein                      |
| AMD    | Age-related macular degeneration              |
| TEM8   | Tumor endothelial marker 8                    |

## Supplementary Information

The online version contains supplementary material available at <https://doi.org/10.1186/s13148-025-01874-4>.

Additional file 1.

## Acknowledgements

Not applicable.

## Author contributions

C.C. and C.G. conducted the experiments and wrote the main manuscript text. C.M. and Y.W. was responsible for mouse experiments and sequencing analysis. Q.W., S.H. and D.L. prepared figures and searched for the literature. Q.Q., T.W., X.W. and C.G. were responsible for coming up with ideas and building the overall framework. Q.Q. and C.G. provided major financial support. All authors reviewed the manuscript.

## Funding

This work has been supported by the National Natural Science Foundation of China (Grant number: 82371072) and Joint Funds for the Innovation of Science and Technology, Fujian Province (Grant number: 2024Y9021).

## Available of data and materials

All data generated or analysed during this study are included in this published article and its supplementary information files.

## Declarations

### Ethics approval and consent to participate

Not applicable.

### Consent for publication

The manuscript is approved by all authors for publication.

### ARVO animal statement

This study strictly adheres to the ARVO animal statement for the use of mice.

### Competing interests

The authors declare that they have no competing interests.

### Author details

<sup>1</sup>Department of Ophthalmology, Tong Ren Hospital, Shanghai Jiao Tong University School of Medicine, Shanghai, People's Republic of China. <sup>2</sup>Department of Ophthalmology, Shanghai General Hospital, Shanghai Jiao Tong University School of Medicine, Shanghai, People's Republic of China. <sup>3</sup>National Clinical Research Center for Eye Diseases; Shanghai Key Laboratory of Ocular Fundus Diseases; Shanghai Engineering Center for Visual Science and Photomedicine, Shanghai Engineering Center for Precise Diagnosis and Treatment of Eye Diseases, Shanghai, People's Republic of China. <sup>4</sup>Department of Ophthalmology, Fuzhou University Affiliated Provincial Hospital, Shengli Clinical College of Fujian Medical University, Fuzhou, Fujian, People's Republic of China. <sup>5</sup>Department of Ophthalmology, Ninth People's Hospital, Shanghai Jiao Tong University School of Medicine, Shanghai, People's Republic of China. <sup>6</sup>Centre for Eye Research Australia, Royal Victorian Eye and Ear Hospital, Melbourne, Australia. <sup>7</sup>Hongqiao International Institute of Medicine, Tongren Hospital, Shanghai Jiao Tong University School of Medicine, Shanghai, People's Republic of China. <sup>8</sup>Department of Ophthalmology, Shigatse People's Hospital, Shigatse, Tibet, People's Republic of China. <sup>9</sup>High Altitude Ocular Disease Research Center of People's Hospital of Shigatse City and Tongren Hospital Affiliated to Shanghai Jiao Tong University School of Medicine, Shanghai, People's Republic of China.

Received: 7 January 2025 Accepted: 8 April 2025

Published online: 17 May 2025

## References

- Du X, Yang L, Kong L, Sun Y, Shen K, Cai Y, et al. Metabolomics of various samples advancing biomarker discovery and pathogenesis elucidation for diabetic retinopathy. *Front Endocrinol (Lausanne)*. 2022;13:1037164.
- Middel CS, Hammes H-P, Kroll J. Advancing Diabetic Retinopathy Research: Analysis of the Neurovascular Unit in Zebrafish. *Cells*. 2021;10(6):1313. <https://doi.org/10.3390/cells10061313>.
- Fung TH, Patel B, Wilmot EG, Amoaku WM. Diabetic retinopathy for the non-ophthalmologist. *Clin Med (Lond)*. 2022;22(2):112–6.
- Lin KY, Hsieh WH, Lin YB, Wen CY, Chang TJ. Update in the epidemiology, risk factors, screening, and treatment of diabetic retinopathy. *J Diabetes Investig*. 2021;12(8):1322–5.
- Constância V, Nunes SP, Henrique R, Jerónimo C. DNA methylation-based testing in liquid biopsies as detection and prognostic biomarkers for the four major cancer types. *Cells*. 2020;9(3):624. <https://doi.org/10.3390/cells9030624>.
- Nishiyama A, Nakanishi M. Navigating the DNA methylation landscape of cancer. *Trends Genet*. 2021;37(11):1012–27.
- Curradi M, Izzo A, Badaracco G, Landsberger N. Molecular mechanisms of gene silencing mediated by DNA methylation. *Mol Cell Biol*. 2002;22(9):3157–73.
- Raciti GA, Desiderio A, Longo M, Leone A, Zatterale F, Prevenzano I, et al. DNA Methylation and Type 2 Diabetes: Novel Biomarkers for Risk Assessment? *Int J Mol Sci*. 2021;22(21):11652. <https://doi.org/10.3390/ijms222111652>.

9. Cai C, Meng C, He S, Gu C, Lhamo T, Draga D, et al. DNA methylation in diabetic retinopathy: pathogenetic role and potential therapeutic targets. *Cell Biosci.* 2022;12(1):186.
10. Desrumaux C, Deckert V, Lemaire-Ewing S, Mossiat C, Athias A, Vandroux D, et al. Plasma phospholipid transfer protein deficiency in mice is associated with a reduced thrombotic response to acute intravascular oxidative stress. *Arterioscler Thromb Vasc Biol.* 2010;30(12):2452–7.
11. Asllanaj E, Zhang X, Ochoa Rosales C, Nano J, Bramer WM, Portilla-Fernandez E, et al. Sexually dimorphic DNA-methylation in cardiometabolic health: a systematic review. *Maturitas.* 2020;135:6–26.
12. Indumathi B, Oruganti SS, Naushad SM, Kutala VK. Probing the epigenetic signatures in subjects with coronary artery disease. *Mol Biol Rep.* 2020;47(9):6693–703.
13. Guay SP, Brisson D, Lamarche B, Gaudet D, Bouchard L. Epipolymorphisms within lipoprotein genes contribute independently to plasma lipid levels in familial hypercholesterolemia. *Epigenetics.* 2014;9(5):718–29.
14. Fcl A. Mitochondrial metabolism and DNA methylation: a review of the interaction between two genomes. *Clin Epigenetics.* 2020;12(1):182.
15. Mittelstaedt NN, Becker AL, Nascimento D, de Freitas RF, Zanin RT, Stein AP, de Souza D. DNA methylation and immune memory response. *Cells.* 2021;10(11):2943. <https://doi.org/10.3390/cells10112943>.
16. Li D, Guo B, Wu H, Tan L, Lu Q. TET family of dioxygenases: crucial roles and underlying mechanisms. *Cytogenet Genome Res.* 2015;146(3):171–80.
17. Ma C, Seong H, Liu Y, Yu X, Xu S, Li Y. Ten-eleven translocation proteins (TETs): tumor suppressors or tumor enhancers? *Front Biosci (Landmark Ed).* 2021;26(10):895–915.
18. Kowluru RA, Shan Y, Mishra M. Dynamic DNA methylation of matrix metalloproteinase-9 in the development of diabetic retinopathy. *Lab Invest.* 2016;96(10):1040–9.
19. Kim YH, Kim YS, Kang SS, Cho GJ, Choi WS. Resveratrol inhibits neuronal apoptosis and elevated Ca<sup>2+</sup>/calmodulin-dependent protein kinase II activity in diabetic mouse retina. *Diabetes.* 2010;59(7):1825–35.
20. Gu C, She X, Zhou C, Su T, He S, Meng C, et al. Dihydroartemisinin ameliorates retinal vascular dysfunction in diabetes mellitus via the FASN/Kmal-mTOR/SREBP1 feedback loop. *Pharmacol Res.* 2021;174: 105871.
21. Wang Y. Study on the pathogenesis of diabetic retinopathy based single-cell sequencing and its clinical risk factors in patients. Shanghai Jiaotong University. 2023.
22. Cai C, Gu C, He S, Meng C, Lai D, Zhang J, et al. TET2-mediated ECM1 hypomethylation promotes the neovascularization in active proliferative diabetic retinopathy. *Clin Epigenetics.* 2024;16(1):6.
23. Lu Y, Brommer B, Tian X, Krishnan A, Meer M, Wang C, et al. Reprogramming to recover youthful epigenetic information and restore vision. *Nature.* 2020;588(7836):124–9.
24. Law PP, Holland ML. DNA methylation at the crossroads of gene and environment interactions. *Essays Biochem.* 2019;63(6):717–26.
25. Mondal AK, Gaur M, Advani J, Swaroop A. Epigenome-metabolism nexus in the retina: implications for aging and disease. *Trends Genet.* 2024;40(8):718–29.
26. Merbs SL, Khan MA, Hackler L Jr, Oliver VF, Wan J, Qian J, et al. Cell-specific DNA methylation patterns of retina-specific genes. *PLoS ONE.* 2012;7(3): e32602.
27. He Y, Dan Y, Gao X, Huang L, Lv H, Chen J. DNMT1-mediated lncRNA MEG3 methylation accelerates endothelial-mesenchymal transition in diabetic retinopathy through the PI3K/Akt/mTOR signaling pathway. *Am J Physiol Endocrinol Metab.* 2021;320(3):E598–e608.
28. Di Y, Wang Y, Wang YX, Wang X, Ma Y, Nie QZ. Maternally expressed gene 3 regulates retinal neovascularization in retinopathy of prematurity. *Neural Regen Res.* 2022;17(6):1364–8.
29. Berdasco M, Gómez A, Rubio MJ, Català-Mora J, Zanón-Moreno V, Lopez M, et al. DNA methylomes reveal biological networks involved in human eye development, functions and associated disorders. *Sci Rep.* 2017;7(1):11762.
30. Gautier T, Deckert V, Nguyen M, Desrumaux C, Masson D, Lagrost L. New therapeutic horizons for plasma phospholipid transfer protein (PLTP): targeting endotoxemia, infection and sepsis. *Pharmacol Ther.* 2022;236: 108105.
31. Sposito AC, Zimetti F, Barreto J, Zanotti I. Lipid trafficking in cardiovascular disease. *Adv Clin Chem.* 2019;92:105–40.
32. Hoekstra M, van der Sluis RJ, Hildebrand RB, Lammers B, Zhao Y, Praticò D, et al. Disruption of phospholipid transfer protein-mediated high-density lipoprotein maturation reduces scavenger receptor bi deficiency-driven atherosclerosis susceptibility despite unexpected metabolic complications. *Arterioscler Thromb Vasc Biol.* 2020;40(3):611–23.
33. Qarawani A, Naaman E, Safuri S, Zayit-Soudry S. Transcriptome Analysis of Amyloid- $\beta$  in the Rat Retina Reveals Important Link to Pathological Processes Implicated in Age-related Macular Degeneration. *Investig Ophthalmol Visual Sci.* 2023;64(8):2734.
34. Yazdanyar A, Jiang XC, Lazzaro D, Brunken W. The Role of Phospholipid Transfer Protein (PLTP) in Lipoprotein Metabolism in the Retina. *Investig Ophthalmol Visual Sci.* 2013;54(15):1374.
35. Lu J, Shi X, Fu Q, Han Y, Zhu L, Zhou Z, et al. New mechanistic understanding of osteoclast differentiation and bone resorption mediated by P2X7 receptors and PI3K-Akt-GSK3 $\beta$  signaling. *Cell Mol Biol Lett.* 2024;29(1):100.
36. Li LF, Gao Y, Xu Y, Su DJ, Yang Q, Liu A, et al. Praeruptorin C alleviates cognitive impairment in type 2 diabetic mice through restoring PI3K/AKT/GSK3 $\beta$  pathway. *Phytother Res.* 2023;37(10):4838–50.
37. Liu Y, Sun Y, Yang J, Wu D, Yu S, Liu J, et al. DNMT1-targeting remodeling global DNA hypomethylation for enhanced tumor suppression and circumvented toxicity in oral squamous cell carcinoma. *Mol Cancer.* 2024;23(1):104.
38. Kundu P, Jain R, Kanuri NN, Arimappamagan A, Santosh V, Kondaiah P. DNA methylation in recurrent glioblastomas: increased TEM8 expression activates the Src/PI3K/AKT/GSK-3 $\beta$ /B-catenin pathway. *Cancer Geno Proteomics.* 2024;21(5):485–501.
39. Cheng Y, Peng L, Deng X, Li T, Guo H, Xu C, et al. Prostaglandin F<sub>2</sub> $\alpha$  protects against pericyte apoptosis by inhibiting the PI3K/Akt/GSK3 $\beta$ /B-catenin signaling pathway. *Ann Transl Med.* 2021;9(12):1021.
40. Shukal D, Bhadresha K, Shastri B, Mehta D, Vasavada A, Johar K Sr. Dichloroacetate prevents TGF $\beta$ -induced epithelial-mesenchymal transition of retinal pigment epithelial cells. *Exp Eye Res.* 2020;197: 108072.
41. Millán I, del Carmen M, Desco I-C, Pérez S, Pulido I, Mena-Mollá S, et al. Pterostilbene Prevents Early Diabetic Retinopathy Alterations in a Rabbit Experimental Model. *Nutrients.* 2019;12(1):82. <https://doi.org/10.3390/nu12010082>.
42. Zhu Y, Wang X, Zhou X, Ding L, Liu D, Xu H. DNMT1-mediated PPAR $\alpha$  methylation aggravates damage of retinal tissues in diabetic retinopathy mice. *Biol Res.* 2021;54(1):25.
43. Kowluru RA, Mohammad G. Epigenetics and mitochondrial stability in the metabolic memory phenomenon associated with continued progression of diabetic retinopathy. *Sci Rep.* 2020;10(1):6655.
44. Xie MY, Yang Y, Liu P, Luo Y, Tang SB. 5-aza-2'-deoxycytidine in the regulation of antioxidant enzymes in retinal endothelial cells and rat diabetic retina. *Int J Ophthalmol.* 2019;12(1):1–7.
45. Meng C, Gu C, He S, Su T, Lhamo T, Draga D, et al. pyroptosis in the retinal neurovascular unit: new insights into diabetic retinopathy. *Front Immunol.* 2021;12: 763092.
46. Antonetti DA, Silva PS, Stitt AW. Current understanding of the molecular and cellular pathology of diabetic retinopathy. *Nat Rev Endocrinol.* 2021;17(4):195–206.
47. Duh EJ, Sun JK, Stitt AW. Diabetic retinopathy: current understanding, mechanisms, and treatment strategies. *JCI Insight.* 2017. <https://doi.org/10.1172/jci.insight.93751>.

## Publisher's Note

Springer Nature remains neutral with regard to jurisdictional claims in published maps and institutional affiliations.